P-25

AN ASSESSMENT AND APPLICATION OF TURBULENCE MODELS FOR HYPERSONIC FLOWS (U)

IN-02-TM

T. J. Coakley
J. R. Viegas
P. G. Huang
M. W. Rubesin

NASA Ames Research Center
Moffett Field, California

Ninth National Aero-Space Plane
Technology Symposium
November 1-2, 1990

Paper No. 106

INTRODUCTION (U)

(U) Accurate Computation of Complex high-speed flows will be an essential ingredient in the successful design of the NASP. The current approach to this computation is to solve the Reynolds averaged Navier-Stokes equations using finite difference methods. An integral part of this approach consists of the development and application of mathematical turbulence models which are necessary in predicting the aerotherodynamic loads on the vehicle and the performance of the propulsion plant. The purpose of this paper is to describe computations of several high speed turbulent flows using various turbulence models and to evaluate the models by comparing computations with the results of experimental measurements. The cases investigated include flows over insulated and cooled flat plates with Mach numbers ranging from 2 to 8 and wall temperature ratios ranging from 0.2 to 1.0. The turbulence models investigated include zero-equation, two-equation and Reynolds-stress transport models.

INTRODUCTION (U)

OBJECTIVE : ACCURATE COMPUTATION OF COMPLEX HIGH-SPEED FLOWS

APPROACH : SOLVE REYNOLDS AVERAGED NAVIER-STOKES EQUATIONS USING TURBULENCE MODELS

PURPOSE : DESCRIBE COMPUTATIONS OF SEVERAL FLOWS AND EVALUATE MODELS BY COMPARISONS WITH EXPERIMENTAL RESULTS

FLOWS : INSULATED AND COOLED FLAT PLATES AT HIGH SPEEDS

MODELS : ZERO-EQUATION, TWO-EQUATION, AND REYNOLDS STRESS MODELS

OUTLINE (U)

(U) This paper is organized as outlined below. It begins with a brief discussion of the types of flows being investigated in our program of identifying and developing successful turbulence models for hypersonic flows at Ames Research Center. Then the basic turbulence models currently under study or planned for future study are discussed. Included in this discussion are the two wall treatments utilized with the models and modifications for compressibility useful in complex flow situations. Numerical aspects of the computations are discussed next. These include numerical grids and boundary conditions, and the numerical methods or codes used with their corresponding turbulence models. The discussion then moves on to a description of the experiments for insulated and cooled plates and continues to a comparison of computations with experimental measurements. The paper ends with a discussion and conclusions based on the results presented and a discussion of future work planned.

OUTLINE (U)

1. TEST FLOWS UNDER STUDY
2. BASIC TURBULENCE MODELS
3. WALL TREATMENTS
4. COMPRESSIBILITY MODIFICATIONS
5. NUMERICAL GRIDS AND BOUNDARY CONDITIONS
6. NUMERICAL METHODS AND MODELS
7. EXPERIMENTS FOR INSULATED AND COOLED PLATES
8. COMPARISONS OF COMPUTATIONS WITH EXPERIMENT
9. DISCUSSION, CONCLUSIONS AND FUTURE WORK

TEST FLOWS UNDER STUDY (U)

(U) Representative test geometries and flows used for comparisons of computation and experiment are shown below. The basic geometries include flat plates, cones and blunt and pointed nose flows. More complicated flows include shock-wave boundary-layer interaction flows arising from impinging shocks, compression ramps and flares. For sufficiently strong shock waves these flows are separated, and it is these cases that pose a strong challenge to the turbulence modeller. Additional flows of interest, but not indicated below, include free shear layers such as jets, wakes and mixing layers, as well as various three-dimensional flows.

TEST MODEL GEOMETRIES USED FOR COMPARISONS OF COMPUTATION AND EXPERIMENT

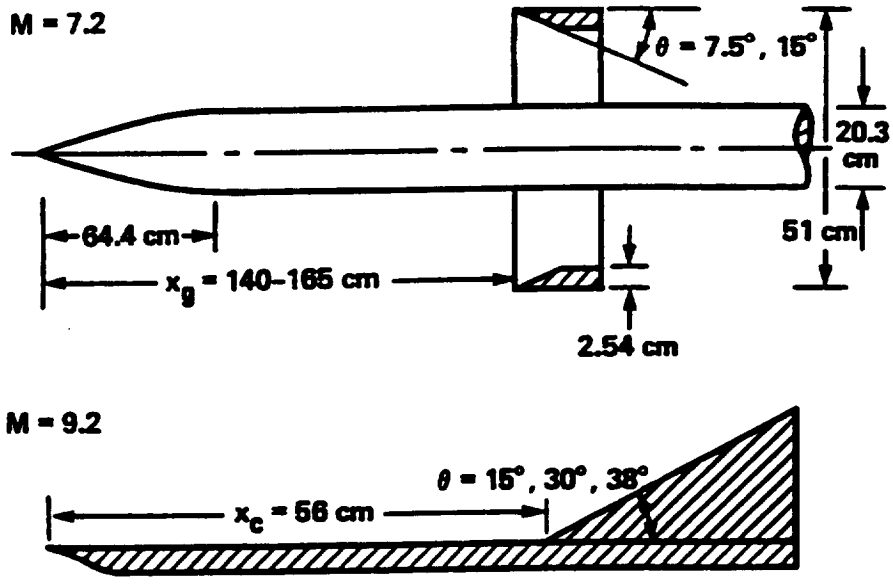

BASIC TURBULENCE MODELS (U)

(U) The basic turbulence models currently under study for NASP applications are listed below. They include zero-, one-, and two-equation eddy viscosity models and Reynolds stress transport models. Six of the models are investigated in the present study and include the Cebeci-Smith zero equation model, the Jones-Launder, Wilcox and Coakley two equation models. These models along with the Johnson-King and Chien models were investigated in an earlier NASP paper, Ref. (14). New to the general investigation of hypersonic flows are the Reynolds stress models, which include two variants of the incompressible model of Launder, Reece and Rodi. These models are the FRAME model (French American Exchange) developed at Ames Research Center and the Launder-Shima model developed at Manchester University. All of the models have been extended to compressible flows from incompressible versions using Favre or mass weighted averaging. Several more turbulence models are also listed in the table and correspond either to models discussed in previous studies or to models of interest in future studies. The open and closed circles indicate which type of wall treatment - either wall dampers or wall functions - was used with each model. For the present study all of the models used wall dampers or the integration-to-the-wall procedure.

BASIC TURBULENCE MODELS (U)

BASIC MODEL		ORIGINATORS	REF	UNDER STUDY AT AMES RES CTR		
				THIS STUDY	PREVIOUS STUDIES	FUTURE STUDIES
ZERO - EQUATION		CEBECI - SMITH	(1)	○	○	
		BALDWIN - LOMAX	(2)		○	
		JOHNSON - KING	(3)		○	○
ONE - EQUATION		BALDWIN - BARTH	(4)			○
TWO - EQUATION	k-ε	JONES - LAUNDER	(5)	○	○ ●	○
	k-ε	CHIEN	(6)		○ ●	
	k-ε	GOLDBERG	(7)			○
	k-ω	WILCOX	(8)	○	○	○
	k-τ	SPEZIALE	(9)			○
	q-ω	COAKLEY	(10)	○	○	○
REYNOLDS STRESS	LRR	FRAME	(11)	○	○	○
	LRR	LAUNDER - SHIMA	(12)	○		○ ●
	MSM	WILCOX	(13)			○
WALL TREATMENTS	○ - WALL DAMPERS			● - WALL FUNCTIONS		

TURBULENCE MODELS - WALL TREATMENTS (U)

(U) The two approaches to wall treatments using turbulence models are discussed more fully below. In the first approach, corresponding to the use of wall damping functions and the procedure of integrating to the wall, strict no-slip boundary conditions are applied to the flow variables at solid surfaces. In this approach, in order to maintain accuracy, it is usually necessary to restrict the first mesh point off the wall to correspond to a value of y+ of the order of one or less. Although this procedure is easy to implement, it has the disadvantage that, with certain codes and/or models, stability problems and slow convergence can be encountered. The alternative approach, that is the use of wall functions based on the law of the wall, is popular and frequently used in incompressible flows. It has the advantage that, because the mesh spacings near the wall can be two orders of magnitude larger than those used with the wall damper approach, the resulting computations are usually more stable and efficient and lead to faster convergence rates. Viegas and Rubesin, Ref. (15), were the first to extend the wall function approach to compressible flows. Most of the applications of this approach to compressible flows have been to insulated walls at Mach numbers equal to 3 or less. In preparing this paper, the wall function approach was incorporated into the high Reynolds number version of the Launder-Shima model. It was found that, although the insulated wall cases were computed with reasonable accuracy, the cooled wall computations were seriously in error. For this reason we have omitted those results here, so that all the models studied in this paper use the wall damper approach.

TURBULENCE MODELS - WALL TREATMENTS (U)

APPROACH	y_1^+ LIMIT	ADVANTAGES	DISADVANTAGES
WALL DAMPING FUNCTIONS (INTEGRATION TO THE WALL)	$y_1^+ \lesssim 1$	EASY TO IMPLEMENT	POSSIBLE STABILITY PROBLEMS AND SLOW CONVERGENCE
WALL FUNCTIONS (LAW OF THE WALL)	$y_1^+ \lesssim 100$	BETTER STABILITY FASTER CONVERGENCE	COMPLICATED WITH ACCURACY PROBLEMS AT HIGH SPEEDS AND COOLED WALLS

COMPRESSIBILITY MODIFICATIONS (U)

(U) It has been our experience that turbulence models developed originally for incompressible flows, when extended to compressible flows, generally give good results for simple cases such as flat plates. This is not the case, however, for more complex flow situations, where the basic turbulence models frequently show serious dissagreement with experimental measurements. In these cases it is advantageous to modify the models to more directly account for compressibility effects and to thus provide better agreement with measurements. Several modifications, which have proven successful in practice, along with their corresponding flow situations and characteristics are listed below. The length scale compression modification was developed originally by Reynolds and Morel and Mansour, Ref. (16), for low speed compressible flows but was found useful for predicting shock induced separation at high speeds by Vuong and Coakley, Ref. (10). The length scale limit, in which the length scale is bounded from below by the Prandtl length scale was found to be useful in predicting heat transfer at reattachment, Ref. (10). Model modifications identified with compressible dissipation and aimed at improving predictions of compressible shear layers at high speeds were developed independently by Zeman and Sarkar, Refs. (17 and 18). Finally, Rubesin has recently developed new modeling for certain compressible pressure-density-strain correlations which are applicable to compressible flows in general, Ref. (19). For the computations of the present study, none of these modifications were used. Limited experimentation on flat plate flows with the first three modifications indicated that the length scale compression and length scale limit modifications gave predictions of CF and CH varying within plus or minus five percent from unmodified model results. The Zeman modification was also tested and, at Mach numbers above about 5, resulted in predictions of CF and CH roughly ten percent below unmodified model results.

COMPRESSIBILITY MODIFICATIONS (U)

NEED: FAILURE OF BASIC MODELS FOR CERTAIN FLOW SITUATIONS

APPROACH: MODIFICATIONS THAT DO NOT COMPROMISE SIMPLE FLOW PREDICTIONS

MODIFICATION/AUTHOR	FLOW SITUATION	CHARACTERISTICS
		$\ell = k^{3/2}/e$, $e = k^*w$
1. LENGTH SCALE COMPRESSION (REYNOLDS, MOREL, MANSOUR)	SHOCK INDUCED SEPARATION	$\frac{d\rho\ell}{dt} = 0$ (in simple compressions)
2. LENGTH SCALE LIMIT (MANSOUR AND OTHERS)	HEAT TRANSFER AT REATTACHMENT	$\ell = \min(2.5y , k^{3/2}/e)$
3. COMPRESSIBLE DISSIPATION (ZEMAN AND SARKAR)	COMPRESSIBLE SHEAR LAYERS AT HIGH SPEEDS	$e \longrightarrow (1 + f(\sqrt{k}/c))^*e$
4. PRESSURE-DENSITY-STRAIN CORRELATIONS (RUBESIN)	COMPRESSIBLE FLOWS IN GENERAL	$\overline{p' u_{i,i}''}$, $\overline{u_{i,i}''}$, $\overline{\rho'\rho'}$

NUMERICAL GRIDS (U)

(U) Typical numerical grids used in our studies are illustrated below. In almost all applications to date an exponentially expanding grid was used in the y direction. In the x direction both uniform and exponential spacing were used for attached flows. For shock-wave boundary-layer interactions and separated flows, uniform spacing was used in the region of interaction as shown. We have recently begun grid refinement studies to establish criteria for grid independent solutions. Some of our results are indicated below. For attached (flat plate) flows we find essentially grid independent solutions can be achieved on relatively coarse grids having about 25 points in the boundary layer. For separated flows (shock-wave boundary layer-interactions) a mesh spacing ratio of 1/4 or less gives grid independent solutions. However, with separated flows we have found significant variations in solutions as the grid is refined in the y direction and have yet to determine criteria for grid independent solutions in this direction.

NUMERICAL GRIDS (U)

Y DIRECTION: EXPONENTIAL SPACING

X DIRECTION: ATTACHED FLOW; UNIFORM - EXPONENTIAL SPACING

SEPARATED FLOW; UNIFORM SPACING - $\Delta x/\delta < 1/4$

GRID REFINEMENT STUDIES (PRIMARILY k - w MODEL)

FLAT PLATE FLOWS - 1% - 2% VARIATIONS IN C_F AND C_H WITH

$0.1 < y_1^+ < 1.0$, $25 <$ Jedge < 90

SEPARATED FLOWS - SMALL VARATIONS WITH $\Delta x/\delta = 1/4 - 1/8$

(UNDER STUDY) - SIGNIFICANT VARIATIONS WITH Jedge = 30, 60, 90

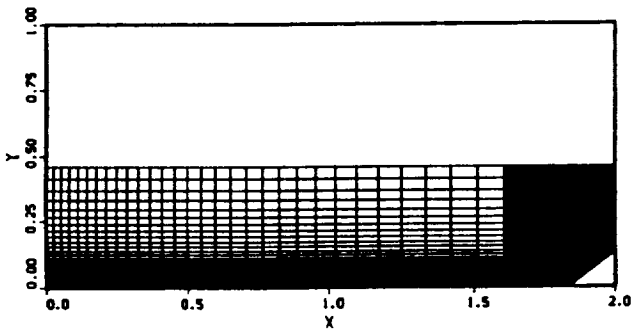

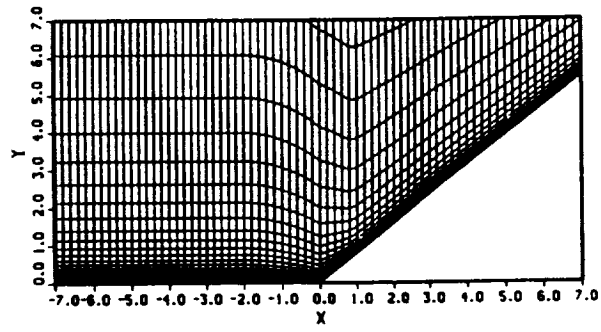

NUMERICAL BOUNDARY CONDITIONS (U)

(U) Numerical boundary conditions used in the computations are summarized below. At solid wall boundaries, no-slip conditions are utilized as indicated. Boundary conditions appropriate to the scale equation (e or w) of the two-equation and Reynolds stress models are also indicated. The proper use of these boundary conditions is frequently critical to the successful application of the model to practical problems. For example, for the k-w model, the use of the lower bound on the solution for w (actually an interior condition rather than a boundary condition), which corresponds to an exact solution of the w equation in the laminar sublayer, is essential for achieving stable and accurate solutions. The formula relating e to the derivative of the turbulent kinetic energy for the L-S model is of a similar nature, also enhancing stability and accuracy. Boundary conditions at the upstream or inflow boundary are also indicated. Free stream conditions are as shown. For some models these free stream conditions can be applied all the way to the wall. For other models, it is necessary to prescribe profiles of velocity, temperature and turbulence variables at the upstream boundary in order to achieve stable solutions. The models corresponding to these two situations are as indicated.

NUMERICAL BOUNDARY CONDITIONS (U)

WALL BOUNDARY :	$u = v = k = \overline{u_i' u_j'} = p_y = 0$,	$T_y = 0$	or	$T = T_{wall}$
$y = 0$	k - e MODEL	$e = 0$		(e - epsilon)
	k - w MODEL	$w \geq 80\nu/y$		(w - omega)
	q - w MODEL	$w_y = 0$		(q - k)
	FRAME MODEL	$e_y = 0$		
	L - S MODEL	$e = 2\nu(\partial\sqrt{k}/\partial y)^2_{y=0}$		

UPSTREAM BOUNDARY : FREE STREAM CONDITIONS u, v, p, T = constant

$x = 0$ $\sqrt{k_\infty}/u_\infty = .001 - .005$, $(\mu_T/\mu) = .01 - 1.0$ (defines e_∞)

PROFILES REQUIRED : k - e , FRAME

PROFILES NOT REQD : k - w , q - w , C - S , L - S

NUMERICAL METHODS AND MODELS (U)

(U) The numerical method/code used with each turbulence model is shown below. The MacCormack 1981 method, Ref.(20), utilizes an explicit - implicit factored ADI proceedure to solve the Reynolds averaged Navier-Stokes equations. The model used with this code is the FRAME Reynolds stress model. The method and code of Coakley 1983, Refs.(21,22), is also a factored ADI proceedure utilizing 2nd order upwind differencing of inviscid fluxes. Models used in this code were all the two-equation models and the Cebeci-Smith zero-equation model. A new code developed by Huang (and Coakley) 1990, which utilizes TVD techniques and a symmetric Gauss-Sidel line relaxation method was used with the L - S model. This code also incorporated several two-equation models including the Chien k-e model and the Coakley q-w model. Solutions obtained with these two models in the Huang code were essentially identical with solutions obtained with the Coakley code. Also shown below are typical Courant numbers (in the x direction) used with each code which are indicative of the relative stability and rate of convergence to steady state solutions.

NUMERICAL METHODS AND MODELS (U)

METHOD/CODE	FEATURES (FINITE VOLUME)	MODELS (THIS STUDY)	COURANT NO. $(u + c)\Delta t/\Delta x$
MACCORMACK 1981	EXPLICIT-IMPLICIT	FRAME	0.1 - 1.0
COAKLEY 1983	UPWIND AF-ADI	TWO EQ. MODELS	1.0 - 10.0
HUANG 1990	TVD SGS RELAXATION	L - S	1.0 - oo

EXPERIMENTS FOR INSULATED AND COOLED PLATES (U)

(U) Results of experimental measurements used in the comparisons with computation are shown below. They were obtained from Ref. (23) and consist of plots of local skin-friction coefficient vs momentum thickness Reynolds number. Also shown is the Karman-Schoenherr correlation curve. The results are shown for both adiabatic (insulated) and non adiabatic (cooled) walls. Since the Karman-Schoenherr curve is based on incompressible measurements, the compressible measurements have been transformed to incompressible form using the van Driest transformation to allow direct comparisons. In this way the effects of Mach number and wall temperature ratios on skin friction are collapsed essentially to a single curve. The numerical computations to be discussed shortly have been similarly transformed. The different symbols on the curves correspond to different Mach numbers, Reynolds numbers, and, where appropriate, wall temperature ratios TW/TAW where TAW is the adiabatic wall temperature. To be consistent with Ref. (23), a recovery factor of 0.9 was used in computing TAW, and a Reynolds analogy factor (2CH/CF) of 1.0 was assumed in deriving a heat transfer correlation from the Karman-Schoenherr skin friction correlation.

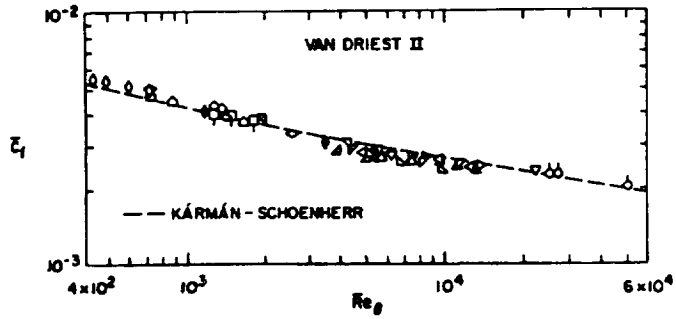

Generalization of adiabatic-wall skin friction measured on flat plates; C_f and Re_θ directly measured; $M_e = 1.5 \rightarrow 5.8$.

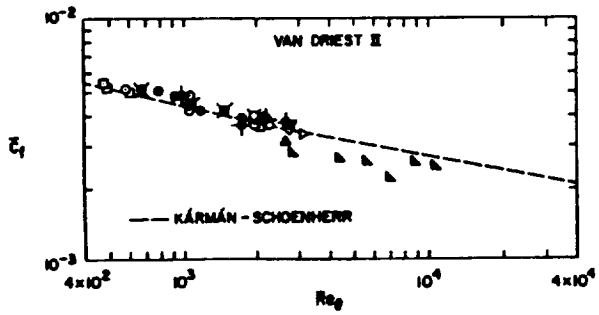

Generalization of nonadiabatic-wall skin friction measured on flat plates; C_f directly measured; $M_e = 2.8 \rightarrow 7.4$.

SKIN FRICTION ON AN ADIABATIC FLAT PLATE (U)

(U) Comparisons of computed and measured skin-friction on insulated plates are shown below and on the next three pages. Shown below are computations using the Cebeci-Smith, k-w and q-w models which are compared with the experimental results discussed on the previous page. It is apparent from these results that all three models give reasonable predictions of skin friction and are within the bounds of experimental error. The most accurate overall agreement is achieved with the k-w model, although best agreement at the highest mach number (of 8) is achieved with the C-S model. The black circles shown on the k-w model results were obtained using a refined grid with Jedge = 60 points, compared with results obtained with the standard grid which had Jedge = 35 points in the boundary layer.

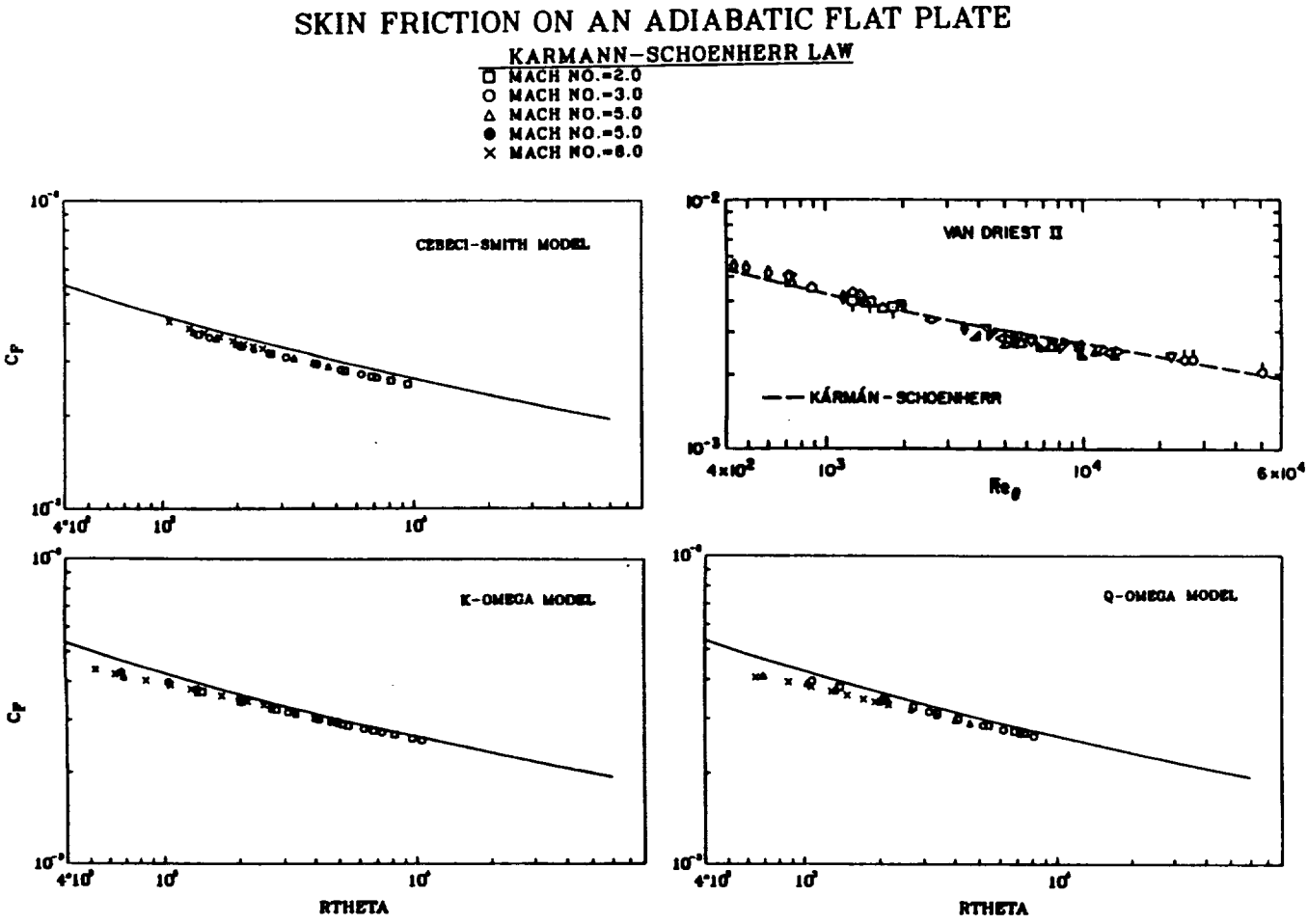

SKIN FRICTION ON AN ADIABATIC FLAT PLATE (U) (CONT)

(U) In the below set of figures, the three additional models are compared with experiment, i.e., the Jones-Launder, Launder-Shima and FRAME models. In these cases, it is found that the FRAME model predictions show very good agreement with experiment, whereas the Jones-Launder and Launder-Shima models show relatively poor agreement. It should be noted that predictions using the FRAME model at a Mach number of 2 are not shown. This was due to the inability of the code to achieve stable solutions at this Mach number. Some difficulty was also encountered at Mach 3, and this is indicated in the figure by the scatter of points (circles). With respect to the Jones-Launder predictions, a systematic departure of solutions with increasing Mach number is observed, whereas with the Launder-Shima model, although all predictions are very consistent in falling on the same curve as the Mach number is varied, the slope of the curve differs substantially from that of the Karman-Schoenherr curve. It is felt that these departures are due to the low-Reynolds-number damping functions of each model and not to any other grid or code-related reason. In this regard, several two-equation models were tested in the Huang code (along with the L-S model), including the Coakley q-w model and the Chien k-e model, and it was found that results obtained were essentially identical with those obtained with the Coakley code. Comparing the predictions of all six models, it appears that the k-w and FRAME models give the best predictions of insulated wall skin friction.

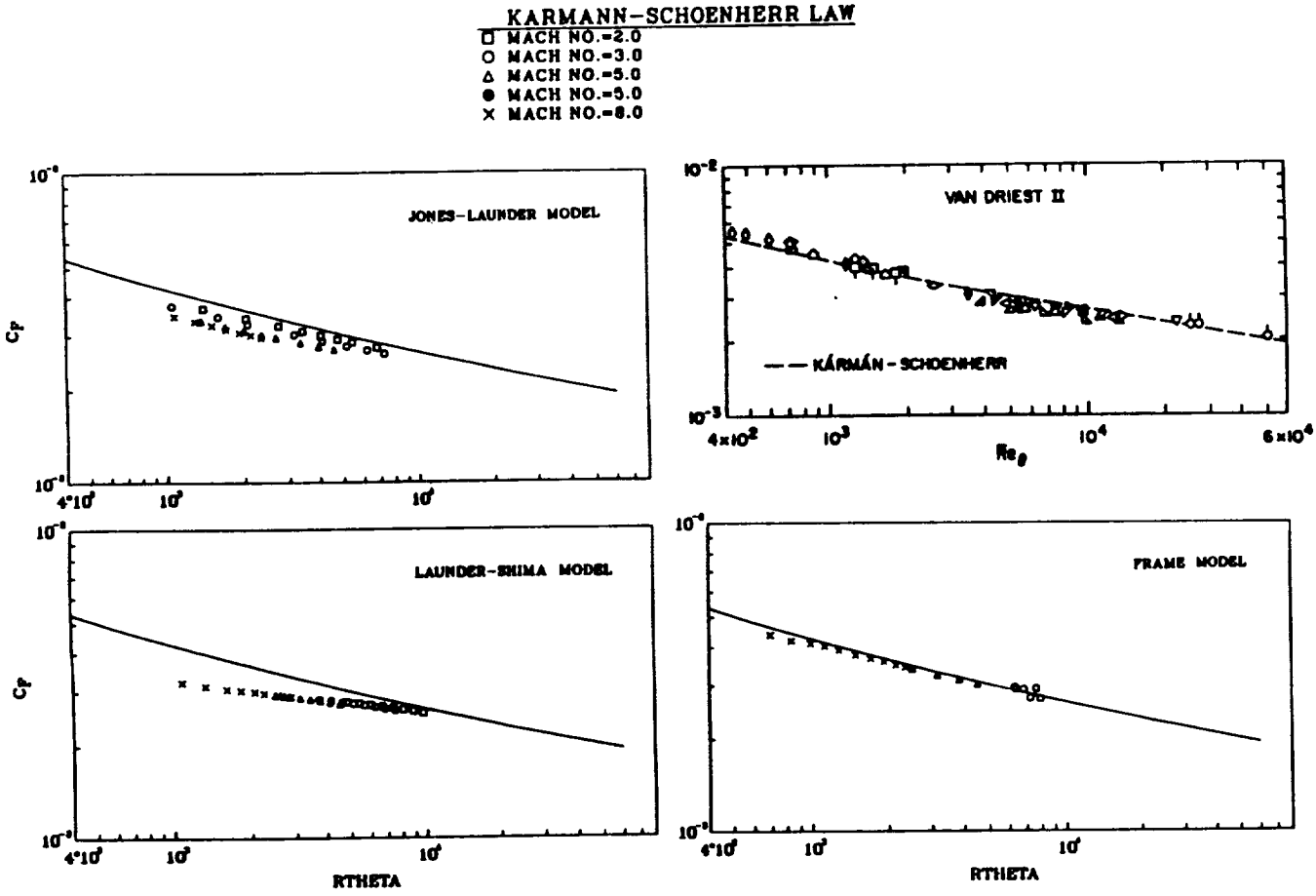

EFFECT OF MACH NUMBER ON ADIABATIC SKIN FRICTION (U)

(U) In the following two sets of figures, the foregoing plots of CF vs RTHETA are replotted as percent variation in skin friction from theory versus Mach number, with individual symbols corresponding to momentum thickness Reynolds number. The conclusions made earlier in comparing the C-S, k-w and q-w models are reconfirmed by the results shown below. The C-S model does best at the highest Mach number, whereas the k-w model is best at the lower three Mach numbers.

EFFECT OF MACH NUMBER ON ADIABATIC SKIN FRICTION ON A FLAT PLATE

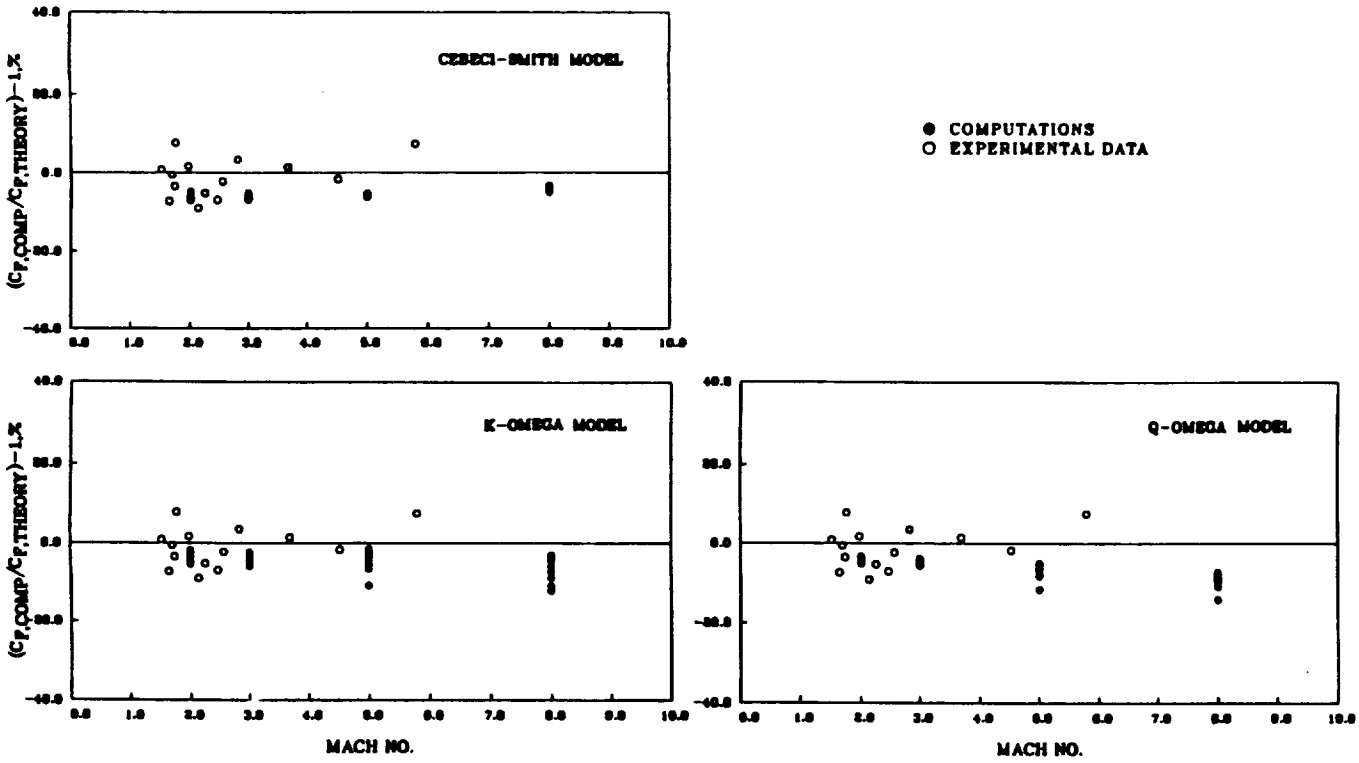

EFFECT OF MACH NUMBER ON ADIABATIC SKIN FRICTION (CONT) (U)

(U) The effect of Mach number on adiabatic skin friction as given by the Jones-Launder, Launder-Shima and FRAME models are shown below. Again, the superiority of the FRAME model results is apparent. It is interesting to note that the Jones-Launder and Launder-Shima models show similar trends with Mach number, i.e., increasing negative variation with increasing Mach number. However, the Jones-Launder model most be considered superior to the Launder-Shima model in that the spread or scatter of points parameterized by the momentum thickness Reynolds number is considerably smaller.

EFFECT OF MACH NUMBER ON ADIABATIC SKIN FRICTION ON A FLAT PLATE

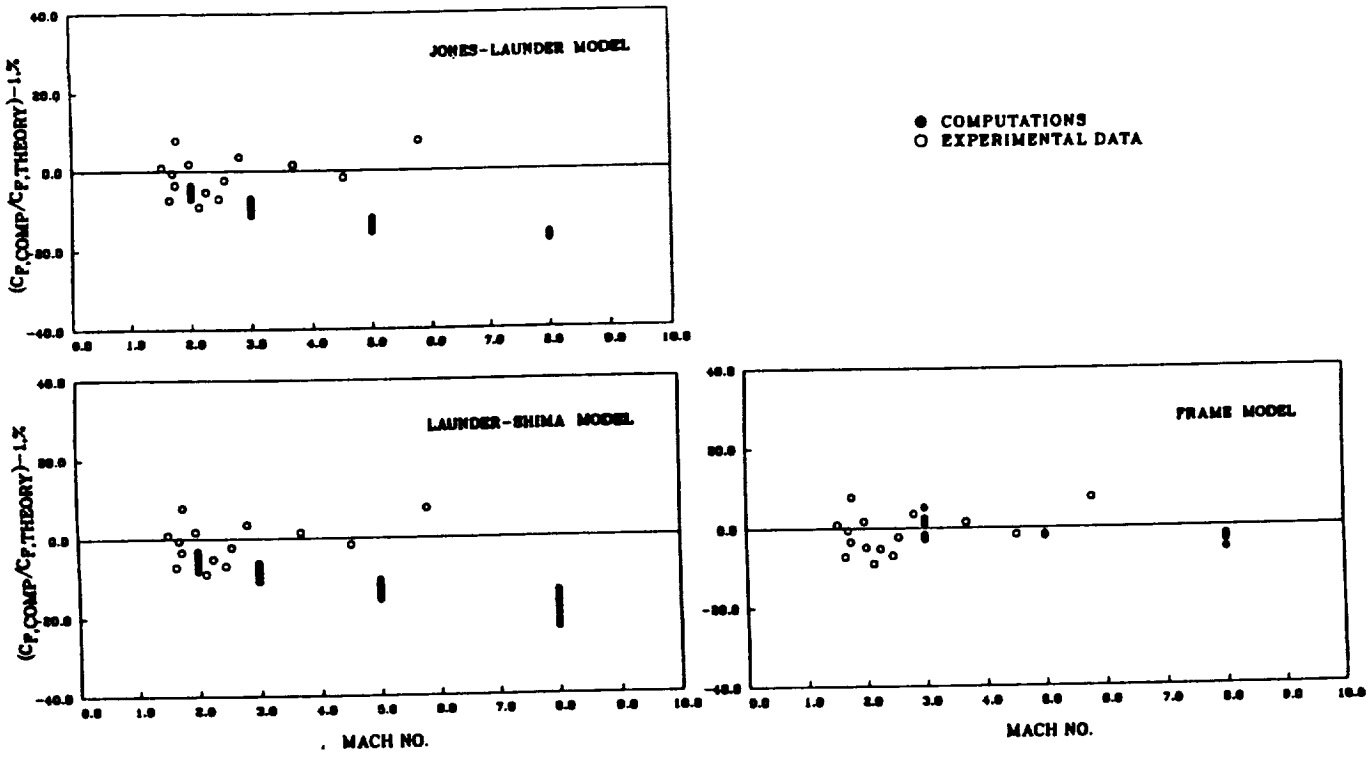

SKIN FRICTION ON A NON-ADIABATIC FLAT PLATE (U)

(U) In the following sets of results, we show comparisons of skin friction and heat transfer with experimental measurements at a Mach number of 5 with varying wall temperature ratios from 0.2 to 0.8. In the first two figures, results for skin friction plotted against momentum thickness Reynolds number are shown. Also shown are the experiemtnal measurements and the Karman-Shoenherr curve. In the results shown below, is apparent that the k-w model gives the best overall agreement with experiment. The Cebeci-Smith and q-w models, although agreeing reasonably well with experiment at the higher temperature ratios, break down at the lowest wall temperature ratio (Tw/Taw = 0.2), with the C-S model predictions falling above the curve and q-w predictions falling below it.

SKIN FRICTION ON A NON-ADIABATIC FLAT PLATE AT MACH NO. = 5

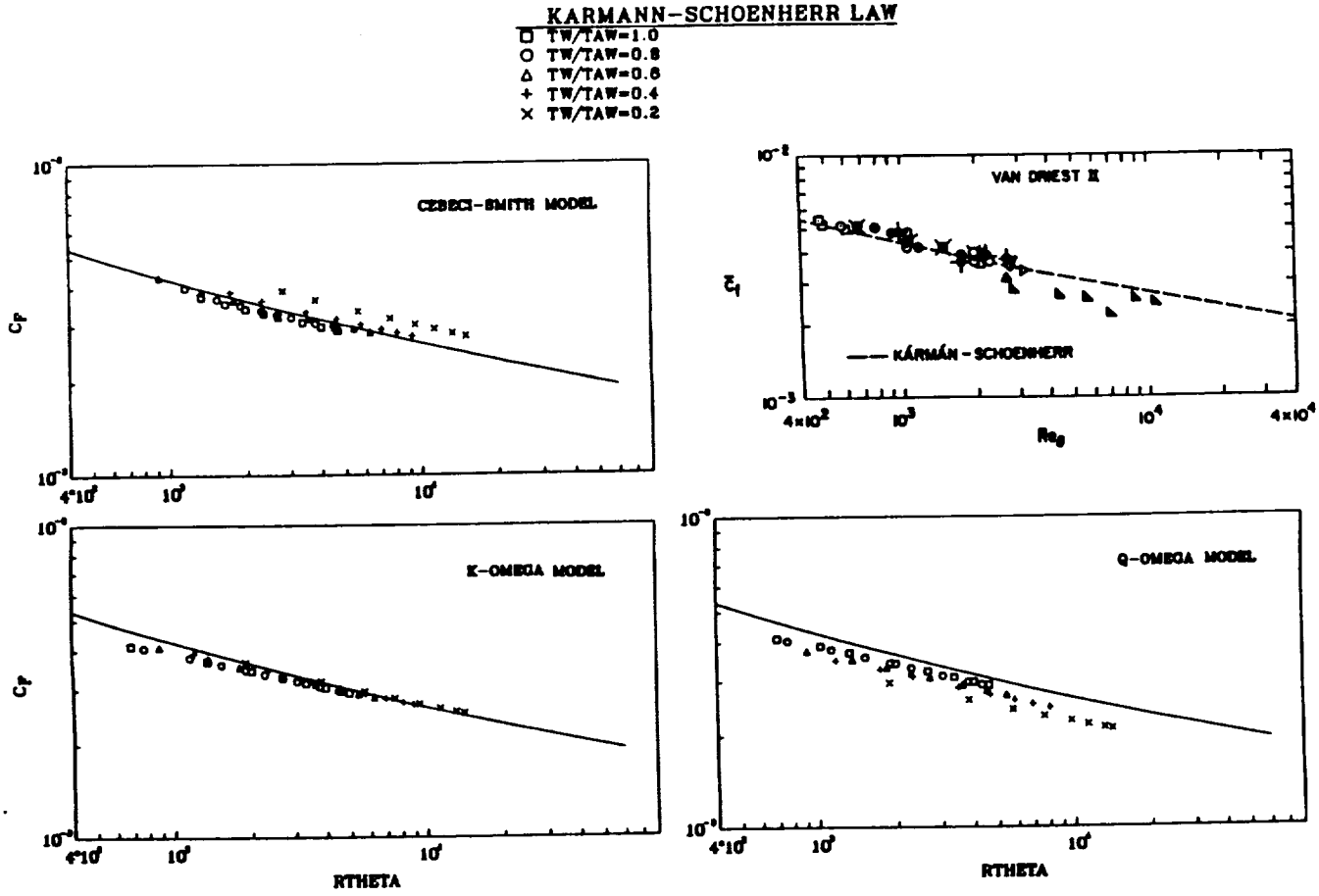

SKIN FRICTION ON A NON-ADIABATIC FLAT PLATE (CONT) (U)

(U) In the comparisons shown below, the Jones-Launder, Launder-Shima and FRAME model predictions are compared with experiment and theory. It is apparent that none of the models give entirely good agreement with theory and experiment, although the departures exhibited by each model are distinctive and different. The Jones-Launder model agrees well at the lowest temperature ratio and departs at the higher ratios. The Launder-Shima model shows a behavior similar to that shown for the adiabatic wall case, that is, small variations with respect to temperature variations but an incorrect slope of CF vs RTHETA. The FRAME model shows negative departures with increasing wall temperatures and was unable to provide prediction of the lowest temperature ratio due to stability problems with the code. With regard to the predictions of all six models, it is apparent that the k-w model gives the best overall agreement.

SKIN FRICTION ON A NON-ADIABATIC FLAT PLATE AT MACH NO. = 5

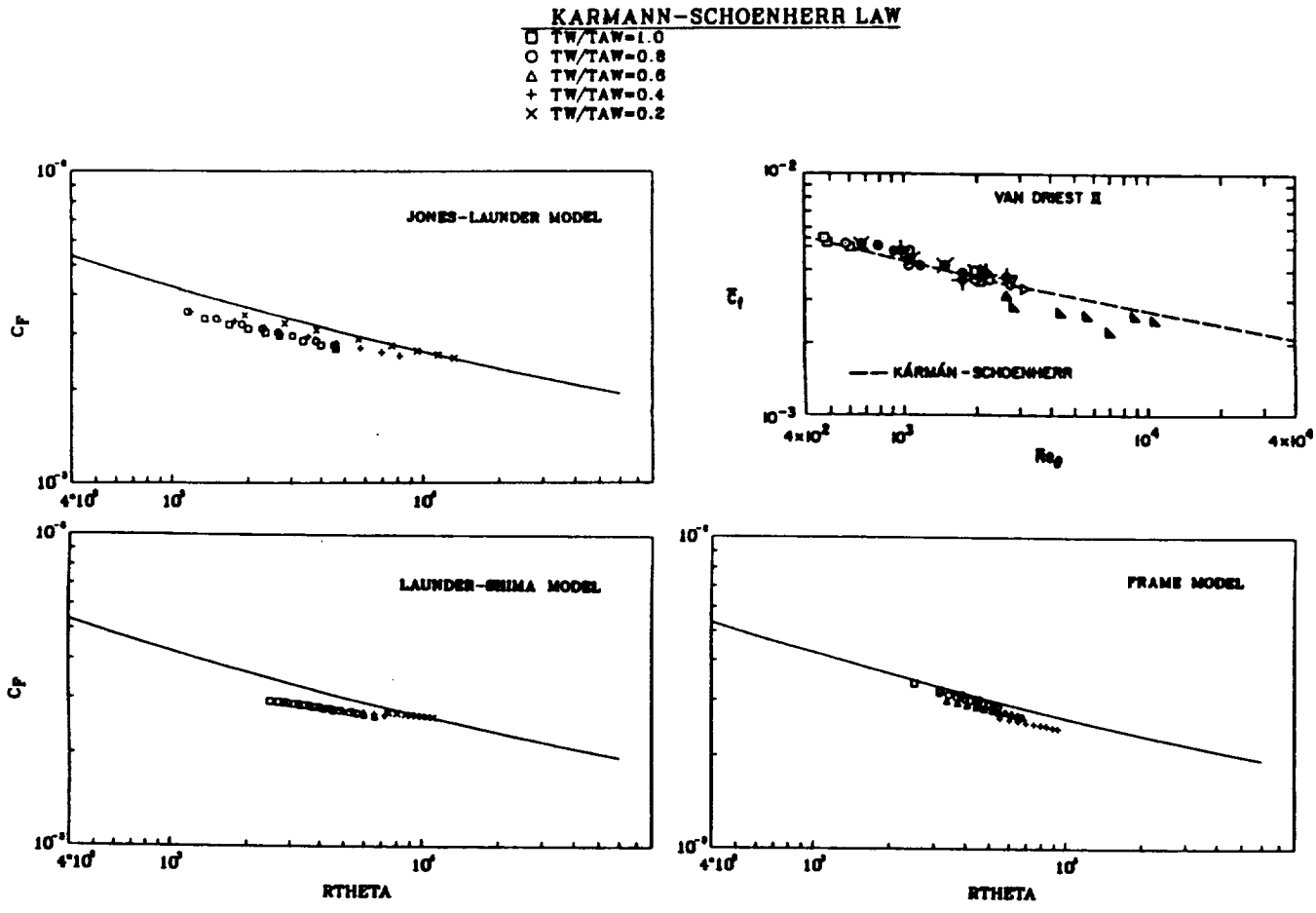

WALL TEMPERATURE EFFECT ON SKIN FRICTION (U)

(U) The results of the previous two figures are replotted in the following two figures with percent variation in CF plotted versus temperature ratio. In the first figure below, we find that the k-w model generally gives the best overall agreement. The breakdown of the Cebeci-Smith model at the lowest temperature ratio is apparent, while the q-w model probably shows the best trend with the data but with a consistent negative error of about 10-15%.

WALL TEMPERATURE EFFECT ON SKIN FRICTION, FLAT PLATE, M=5

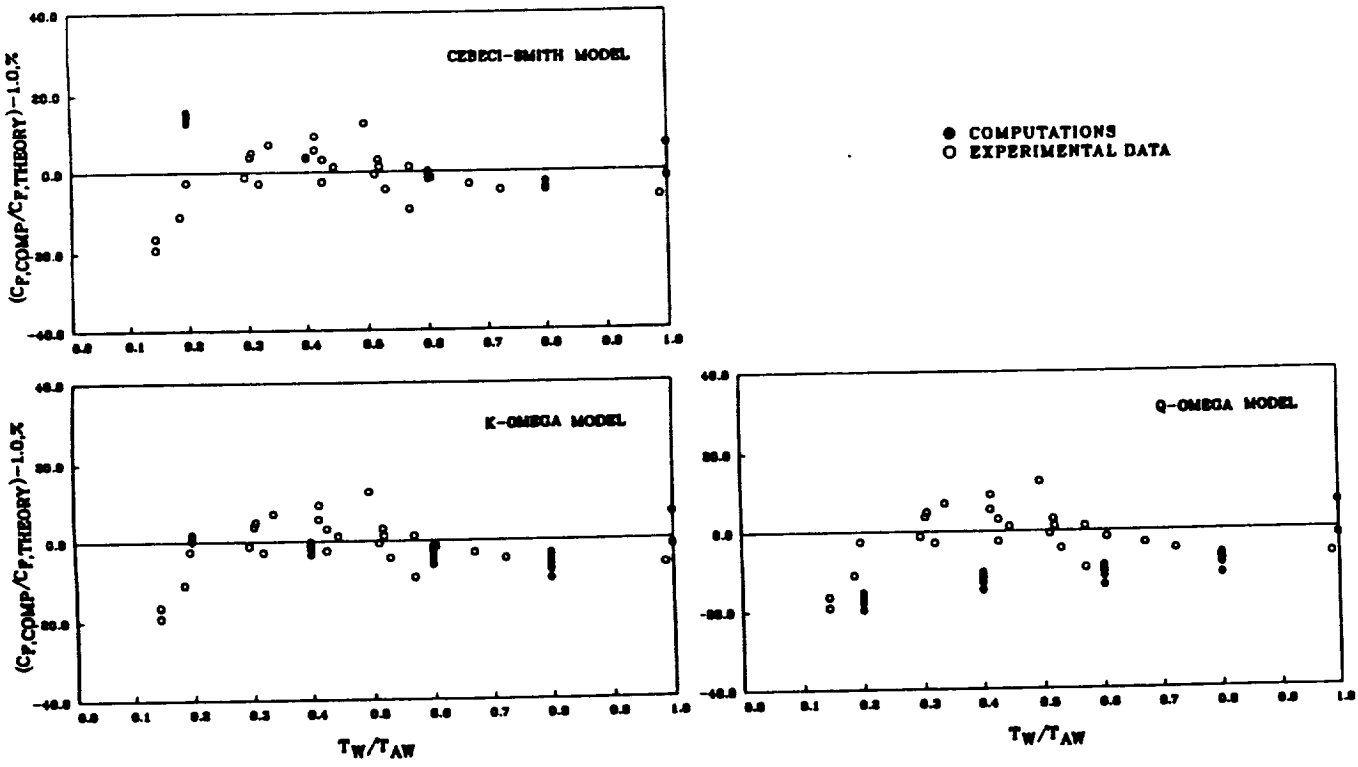

WALL TEMPERATURE EFFECT ON SKIN FRICTION (CONT) (U)

(U) The effect of wall temperature on skin friction at M=5 using the Jones-Launder, Launder-Shima and FRAME models are shown in the following figure. In these cases, the Jones-Launder and Launder-Shima models give the best agreement at the lowest temperature ratios but depart significantly from experiment at the higher ratios. The FRAME model also shows significant departures from experiment. It is apparent from these two sets of plots that the k-w model gives the best overall agreement with experiment followed by the FRAME model.

WALL TEMPERATURE EFFECT ON SKIN FRICTION, FLAT PLATE, M=5

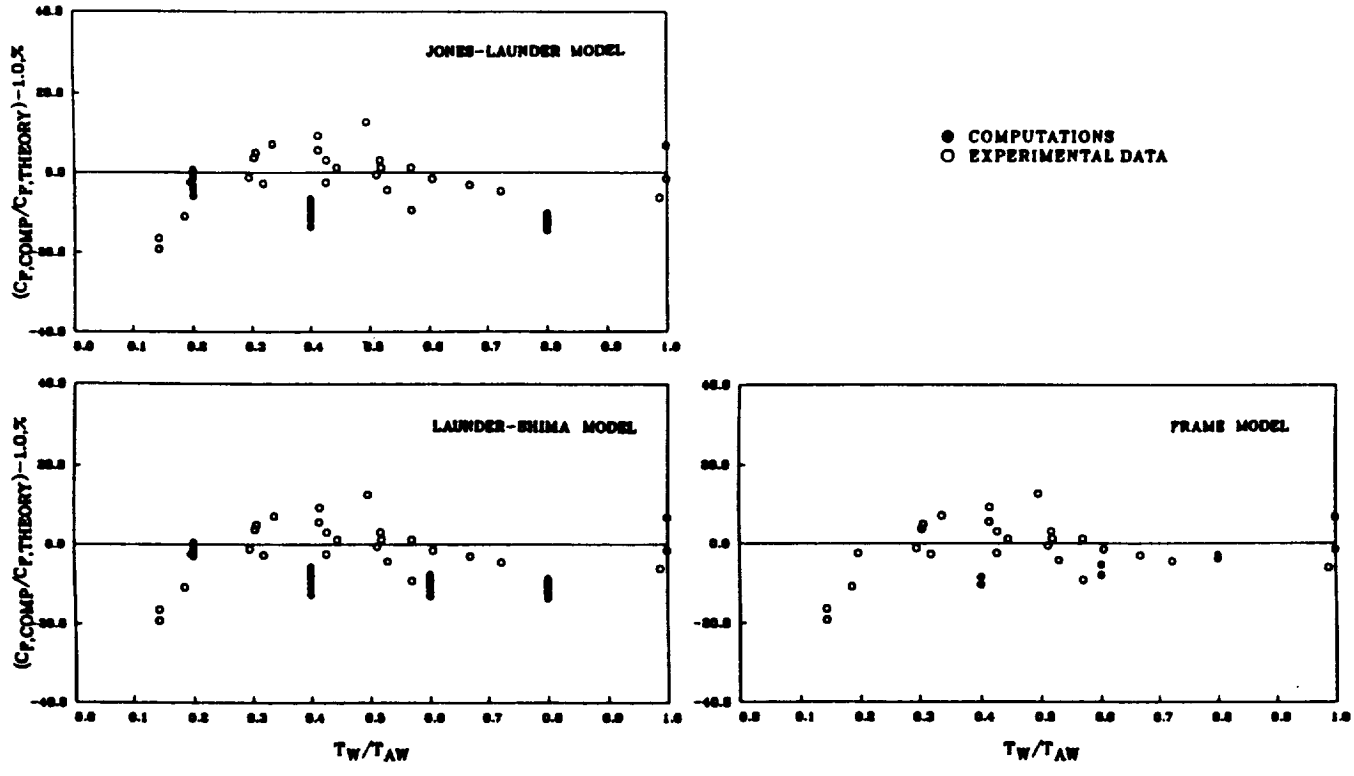

WALL TEMPERATURE EFFECT ON STANTON NUMBER (U)

(U) The effect of wall temperature on heat transfer at M=5 is shown on the next two figures. In these figures, the percent variation in Stanton number is plotted versus wall temperature ratio. In the first figure shown below, we find that the q-w model gives the best overall agreement with measurement and theory, while the Cebeci-Smith model gives the worst agreement. The k-w model gives results intermediate between the other two models. Although it gives the worst agreement, the C-S model does show the smallest variation with momentum thickness Reynolds number (i.e., the spread of individual symbols), and this could be an advantage if modifications to the model could be found to improve the basic agreement and trends.

WALL TEMPERATURE EFFECT ON STANTON NUMBER, FLAT PLATE, M=5

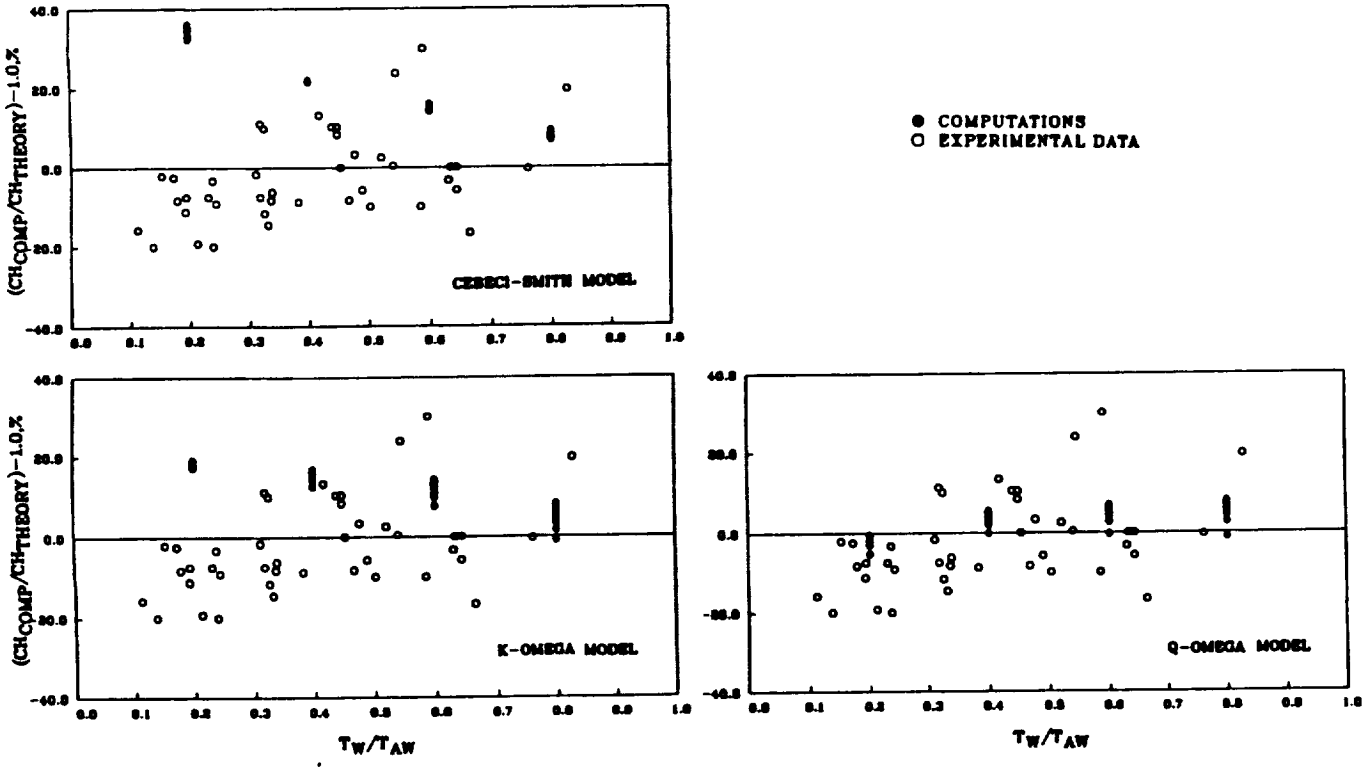

WALL TEMPERATURE EFFECT ON STANTON NUMBER (CONT) (U)

(U) The effect of wall temperature on Stanton number at M=5 using the additional three models is shown in the figure below. Here we find that none of the models show very good agreement with experiment. The FRAME model shows the greatest departures from theory/correlation but gives the correct trend with wall temperature. The Jones-Launder and Launder-Shima models show smaller (but still large) departures but have large spreads with respect to Reynolds number. It is clear that the best overall model in predicting heat transfer is the q-w model.

WALL TEMPERATURE EFFECT ON STANTON NUMBER, FLAT PLATE, M=5

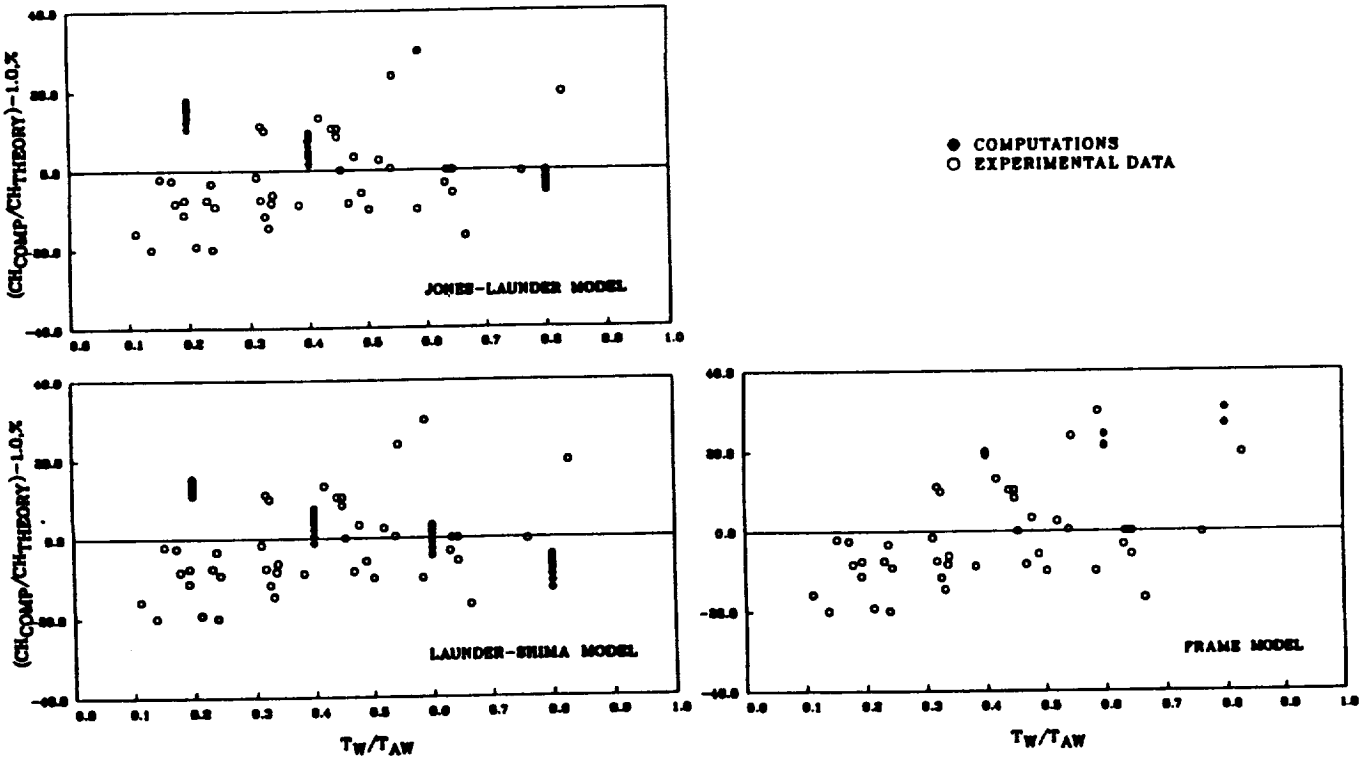

CONCLUSIONS (U)

(U) A summary of the basic results discussed previously is given below. For skin friction on insulated plates, the Jones-Launder and Launder-Shima models show poorest agreement, while the k-w and FRAME models show best agreement, well within the experimental scatter. The Cebeci-Smith and q-w models also show good agreement. For skin friction on cooled plates, the calculations show greater departures, especially at the lowest wall temperatures. The best performing model in this case is the k-w model. The poorest performers were the q-w and Launder-Shima models. It is interesting to note that, although the L-S model is dificient in predicting the correct slope of the CF vs RTHETA curves, it is the most consistent; that is, the computed points lie closest to a single line. Thus, if the model can be improved by predicting the correct slope, it may give the most accurate overall predictions. For heat transfer to cooled plates, the Cebeci-Smith and FRAME models show the greatest departures from experiment, while the q-w model shows the least.

CONCLUSIONS (U)

1. FOR SKIN FRICTION ON INSULATED PLATES
   a. J-L & L-S MODELS SHOW POOREST AGREEMENT
   b. k-w & FRAME MODELS SHOW BEST AGREEMENT
2. FOR SKIN FRICTION ON COOLED PLATES
   a. C-S, q-w, J-L & L-S MODELS SHOW POOREST AGREEMENT
   b. k-w MODEL SHOWS BEST AGREEMENT
3. L-S MODEL SHOWS MOST CONSISTENT RESULTS BUT GIVES INCORRECT SLOPE TO CURVES OF CF VS RTHETA
4. FOR HEAT TRANSFER TO COOLED PLATES
   a. C-S & FRAME MODELS SHOW POOREST AGREEMENT
   b. Q-W MODEL SHOWS BEST AGREEMENT

FUTURE WORK (U)

(U) A partial list of tasks to be completed in the future is listed below. One of the first tasks will be to improve predictions of the Launder-Shima model, probably by modifying the low Reynolds number damping functions. Closely allied with this task will one to test the FRAME model in the Huang code to resolve and eliminate any purely numerical differences, some of which might be the source of the poor L-S predictions. One of the most important tasks will be to complete the grid refinement studies of separated shock-wave boundary-layer interaction flows. As noted in the paper, significant variations in solutions with respect to grid point spacing in the normal direction have been found, and these must be understood and resolved. Although not reported here, considerable work has been done with wall functions for high speed flows, but they have been found to be especially deficient for highly cooled walls. We hope to remove these deficiencies in the future. Additional tasks include improvements in the Johnson-King (zero-equation) model for hypersonic flows, and testing of several additional models which are of interest. These are the recently developed Baldwin-Berth one-equation model, the two-equation models of Speziale and Goldberg, and the multi-scale Reynolds stress model of Wilcox. Coincident with the above tasks with be applying our best models to the computation of additional test flows.

FUTURE WORK (U)

1. IMPROVE LAUNDER-SHIMA MODEL
2. TEST FRAME MODEL IN HUANG CODE
3. CONTINUE GRID REFINEMENT STUDIES OF SEPARATED FLOWS
4. RUN REYNOLDS STRESS MODELS ON SEPARATED FLOWS
5. IMPROVE WALL FUNCTIONS FOR COOLED WALLS
6. IMPROVE JOHNSON-KING MODEL FOR HYPERSONIC FLOWS
7. TEST BALDWIN-BARTH, SPEZIALE, GOLDBERG & WILCOX M.S. MODELS
8. RUN ADDITIONAL TEST FLOWS WITH BEST MODELS

REFERENCES

(U) 1. Cebeci, T. and Smith, A. M. O., Analysis of Turbulent Boundary Layers, Academic Press,1974, pp. 211-257.

(U) 2. Baldwin, B. S. and Lomax, H., "Thin Layer Approximation and Algebraic Model for Separated Turbulent Flows," AIAA Paper 78-257, Jan. 1978.

(U) 3. Johnson, D. A. and King, L. S., "A Mathematically Simple Turbulence Closure Model for Attached and Separated Turbulent Boundary Layers," AIAA Journal, Vol. 23, Nov. 1985, pp. 1684-1692.

(U) 4. Baldwin, B. S. and Barth, T. J., "A One Equation Turbulence Model for High Reynolds Number Wall-Bounded Flows," NASA Technical Memorandum 102847, Aug. 1990.

(U) 5. Jones, W. P. and Launder, B. E., The Prediction of Laminarization with a Two-Equation Model of Turbulence," Int. J. of Heat and Mass and Mass Transf., Vol. 15, Feb. 1972, pp. 301-314.

(U) 6. Chien, K. Y., "Predictions of Channel and Boundary Layer Flows with a Low-Reynolds-Number Turbulence Model," AIAA Journal, Vol. 20, Jan. 1982, pp. 33-38.

(U) 7. Goldberg, U. and Ota, D., "A k- Near-Wall Formulation for Separated Flows," AIAA Paper 90-1482, June 1990.

(U) 8. Wilcox, D. C., "Reassessment of the Scale-Determining Equation for Advanced Turbulence Models," AIAA Journal, Vol. 26, Nov. 1988, pp. 1299-1310.

(U) 9. Speziale, C. G., Abid, R., Anderson, E. C., "A Critical Evaluation of Two-Equation Models for Near Wall Turbulence," AIAA Paper 90-1481, June 1990.

(U) 10. Voung, S. T. and Coakley, T. J., "Modeling of Turbulence for Hypersonic Flows with and without Separation," AIAA Paper 87-0286, Jan. 1987.

(U) 11. Vandromme, D. D., Ha Minh, H., Viegas, J. R. and Rubesin, M. W., "Second Order Closure for the Calculation of Compressible Wall Bounded Flows with an Implicit Navier-Stokes Solver," 4th Symp. on Turbulent Shear Flows, Karlsruhe, F. R. Germany, 1983.

(U) 12. Launder, B. E. and Shima, N., "Second-Moment Closure for the Near-Wall Sublayer: Development and Application," AIAA Journal, Vol. 27, Oct. 1989, pp. 1319-1325.

REFERENCES (CONT.)

(U) 13. Wilcox, D. C., "Multiscale Model for Turbulent Flows," AIAA Journal, Vol. 26, Nov. 1988, pp. 1311-1319.

(U) 14. Coakley, T. J. and Huang, P. G., "Evaluation of Turbulence Models for Hypersonic Flows," Paper 24, 8th NASP Symposium, Monterey, CA, 1990.

(U) 15. Viegas, J. R. amd Rubesin, M. W., "On the Use of Wall Functions as Boundary Conditions for Two-Dimensional Separated Compressible Flows," AIAA Paper 85-0180, Jan. 1985.

(U) 16. Morel, T. and Mansour, N. N., "Modeling of Turbulence in Internal Combustion Engines," SAE Technical Paper Series 820040, Feb. 1982.

(U) 17. Zeman, O., "Dilitation dissipation: The concept and application in modeling compressible mixing layers," Phys. Fluids A., Vol. 2, Feb. 1990.

(U) 18. Sarkar, S. and Balakrishnan, L., "Application of a Reynolds Stress Turbulence Model to the Compressible Shear Layer," NASA Contractor Report 182002, Feb. 1990.

(U) 19. Rubesin, M. W., "Extra Compressibility Terms for Favre-Averaged Two-Equation Models of Inhomogeneous Turbulent Flows," NASA Contractor Report 177556, June 1990.

(U) 20. MacCormack, R. W., "A Numerical Method for Solving the Equation of Compressible Viscous Flow," AIAA Paper 81-0110, Jan. 1981.

(U) 21. Coakley, T. J., "Turbulence Modeling Methods for the Compressible Navier-Stokes Equations," AIAA Paper 83-1693, July 1983.

(U) 22. Coakley, T. J., "A Compressible Navier-Stokes Code for Turbulence Flow Modeling," NASA TM-85899, 1984.

(U) 23. Hopkins, E. J. and Inouye, M., "An Evaluation of Theories for Predicting Turbulent Skin Friction and Heat Transfer on Flat Plates at Supersonic and Hypersonic Mach Numbers," AIAA Journal, Vol. 9, June 1971, pp. 993-1003.